1521-009X/47/4/350–357$35.00
DRUG METABOLISM AND DISPOSITION

https://doi.org/10.1124/dmd.118.084988
Drug Metab Dispos 47:350–357, April 2019

A Comparison of Total and Plasma Membrane Abundance of Transporters in Suspended, Plated, Sandwich-Cultured Human Hepatocytes Versus Human Liver Tissue Using Quantitative Targeted Proteomics and Cell Surface Biotinylation[S]

Vineet Kumar, Laurent Salphati, Cornelis E. C. A. Hop, Guangqing Xiao,[1] Yurong Lai, Anita Mathias, Xiaoyan Chu, W. Griffith Humphreys,[2] Mingxiang Liao,[3] Scott Heyward, and Jashvant D. Unadkat

Department of Pharmaceutics, University of Washington, Seattle, Washington (V.K., J.D.U.); Drug Metabolism and Pharmacokinetics, Genentech, South San Francisco, California (L.S., C.E.C.A.H.); Drug Metabolism and Pharmacokinetics, Biogen Idec, Cambridge, Massachusetts (G.X.); Departments of Clinical Research, Clinical Pharmacology, and Drug Metabolism and Pharmacokinetics, Gilead Sciences, Foster City, California (Y.L., A.M.); Department of Pharmacokinetics, Pharmacodynamics, and Drug Metabolism, Merck & Co., Kenilworth, New Jersey (X.C.); Bristol-Myers Squibb, Princeton, New Jersey (W.G.H.); Takeda Pharmaceuticals International, Cambridge, Massachusetts (M.L.); and BioIVT, Baltimore, Maryland (S.H.)

Received October 18, 2018; accepted January 7, 2019

ABSTRACT

Suspended (SH), plated (PH), and sandwich-cultured hepatocytes (SCH) are commonly used models to predict in vivo transporter-mediated hepatic uptake (SH or PH) or biliary (SCH) clearance of drugs. When doing so, the total and the plasma membrane abundance (PMA) of transporter are assumed not to differ between hepatocytes and liver tissue (LT). This assumption has never been tested. In this study, we tested this assumption by measuring the total and PMA of the transporters in human hepatocyte models versus LT (total only) from which they were isolated. Total abundance of OATP1B1/2B1/1B3, OCT1, and OAT2 was not significantly different between the hepatocytes and LT. The same was true for the PMA of these transporters across the hepatocyte models. In contrast, total abundance of the sinusoidal efflux transporter, MRP3, and the canalicular efflux transporters, MRP2 and P-gp, was significantly greater ($P < 0.05$) in SCH versus LT. Of the transporters tested, only the percentage of PMA of OATP1B1, P-gp, and MRP3, in SCH (82.8% ± 7.3%, 57.5% ± 10.9%, 69.3% ± 5.7%) was significantly greater ($P < 0.05$) than in SH (73.3% ± 6.4%, 27.4% ± 6.4%, 53.6% ± 4.1%). If the transporters measured in the plasma membrane are functional and the PMA in SH is representative of that in LT, these data suggest that SH, PH, and SCH will result in equal prediction of hepatic uptake clearance of drugs mediated by the transporters tested above. However, SCH will predict higher sinusoidal efflux and biliary clearance of drugs if the change in PMA of these transporters is not taken into consideration.

Introduction

The liver, by either hepatic uptake/efflux transport or metabolism or both, predominately clears the majority of small-molecule drugs on the market or in development. Predicting in vivo hepatobiliary clearances of new molecular entities is important to predict their first in human dose, potential drug–drug interactions and the impact of genetic polymorphism of transporters/enzymes on their disposition. If the liver is the target organ for drug therapy, such predictions could also help estimate the hepatic exposure of a drug at a given dosage regimen.

Several hepatocyte models are commonly used to predict in vivo hepatobiliary clearance of drugs. Suspended (SH) or plated hepatocytes (PH) are used to predict in vivo hepatic uptake clearance of drugs, whereas sandwich-cultured hepatocytes (SCH) are used to predict both in vivo uptake and biliary clearance (CL_b) of drugs. Although these hepatocyte models have been successfully used to predict in vivo metabolic clearance (CL) of drugs (Naritomi et al., 2003; Soars et al., 2007), they have been shown to severely underpredict the in vivo transporter-mediated CL of drugs (Abe et al., 2008; Jones et al., 2012; Zou et al., 2013). One possible reason for this underprediction could be a difference in hepatic transporter abundance (total and/or plasma membrane) between hepatocyte models and liver tissue (LT). Indeed, we have previously shown this to be the case in the rat SCH versus LT (Ishida et al., 2018). Taking into consideration such difference in the total transporter abundance (SCH vs. LT) enabled us to successfully predict rosuvastatin hepatic uptake CL in rats determined by positron

V.K. was supported in part by the Simcyp Grant and Partnership Scheme and University of Washington Research Affiliate Program on Transporters funded by Genentech, Biogen, Gilead, Merck, Bristol-Meyers Squibb, Pfizer, and Takeda. This work will constitute part of the thesis of VK.

[1]Current affiliation: Takeda Pharmaceuticals International, Cambridge, Massachusetts.
[2]Current affiliation: Aranmore Pharma Consultant, Trenton, New Jersey.
[3]Current affiliation: Clovis Oncology, San Francisco, California.
https://doi.org/10.1124/dmd.118.084988.
[S]This article has supplemental material available at dmd.aspetjournals.org.

ABBREVIATIONS: CL_b, biliary clearance; DTT, dithiothreitol; IVIVE, in vitro to in vivo extrapolation; LC-MS/MS, liquid chromatography–tandem mass spectrometry; LT, liver tissue; PH, plated hepatocytes; PHL, pooled human liver; PMA, plasma membrane abundance; SCH, sandwich-cultured hepatocytes; SH, suspended hepatocytes.

emission tomography imaging (Ishida et al., 2018). Therefore, to investigate whether the same was true for human hepatocytes, we determined the total and the plasma membrane transporter abundance in the hepatocyte models versus human LT (total only) using targeted quantitative proteomics. To do so, we included the following unique design features not hitherto implemented by others: 1) the abundance of hepatic transporters in the hepatocyte models was compared with the LT from which the hepatocytes were isolated; 2) the percentage of plasma membrane abundance (PMA) of hepatic transporters was quantified in the hepatocyte models using a cell surface biotinylation method optimized in our laboratory; 3) to avoid interindividual variability in the total membrane isolation (a method routinely used by us and others), the total abundance of transporters was quantified in the homogenate (not total membrane) of human liver tissues and hepatocytes. In this work, we present data from these studies, which can guide selection of the appropriate hepatocyte model to predict in vivo hepatic uptake and biliary efflux CL of drugs.

Materials and Methods

Chemicals and Reagents

Synthetic signature peptides for OATP1B1, OATP2B1, OATP1B3, NTCP, OCT1, OAT2, MRP3, MRP2, P-gp, and BSEP were obtained from New England Peptides (Boston, MA). The corresponding stable isotope-labeled peptides for above transporters and Na^+-K^+ ATPase, dithiothreitol (DTT), iodoacetamide, mass spectrometry grade trypsin, William's E medium (no glutamine), cryopreserved hepatocyte recovery medium, total protein quantification bicinchoninic acid assay kit, Hanks' balanced salt solution with calcium and magnesium, and Pierce cell surface protein isolation kit were obtained from Thermo Scientific (Rockford, IL). Pierce cell surface protein isolation kit contains sulfosuccinimidyl-2-(biotinamido) ethyl-1, 3-dithiopropionate, quenching solution (100 mm glycine), lysis buffer, neutravidin agarose gel, wash buffer, column accessory pack, DTT, phosphate buffer, and Tris buffer. High-pressure liquid chromatography–grade acetonitrile and SDS were purchased from Fischer Scientific (Fair Lawn, NJ). Formic acid was purchased from Sigma-Aldrich (St. Louis, MO). All reagents were analytical grade. Twenty-four–well collagen-coated plates and matrigel were purchased from Corning (Kennebunk, ME). Human hepatocyte thaw medium, INVITROGRO CP medium, INVITROGRO HI medium, and TORPEDO antibiotic mix were obtained from BioIVT (Westbury, NY).

Procurement of Human Liver Tissues and Hepatocytes

Human liver frozen tissues (about 150–250 mg, $n = 4$) and cryopreserved human hepatocytes isolated from the respective human liver tissues were obtained from BioIVT. The demographics of the human liver donors are shown in Supplemental Table 1.

Homogenate Preparation of Human Liver Tissue and Hepatocytes (SH, PH, and SCH) To Quantify Total Transporter Abundance

LT. About 50–100 mg human liver tissue from each donor was homogenized in extraction buffer II (Pierce cell surface protein isolation kit) in Omni Bead Ruptor at 4°C. The homogenized liver tissue was dissolved in extraction buffer II and 2% SDS (1:1) for protein quantification by liquid chromatography–tandem mass spectrometry (LC-MS/MS) analyses.

SH. Cryopreserved human hepatocytes were partially thawed at 37°C and then quickly transferred to a 15-ml tube containing 5 ml cryopreserved hepatocyte recovery medium (4°C). After centrifugation at 1000*g* for 5 minutes at 4°C, the cryopreserved hepatocyte recovery medium was aspirated, and 5 ml William's E medium (37°C) was added to the hepatocytes. The live hepatocytes were counted using the trypan blue exclusion method. About 8.4×10^6 viable hepatocytes were transferred to a 15-ml tube containing Hanks' balanced salt solution buffer and incubated at 37°C for 30 minutes. Then the hepatocytes were pelleted by centrifuging the tube at 1000*g* for 5 minutes at 4°C. The pellet was dissolved in extraction buffer II and 2% SDS (1:1) for protein quantification by LC-MS/MS analyses.

PH. About 0.35×10^6 hepatocytes were plated per well in a 24-well collagen-coated plate for 5 hours with 0.5 ml/well TORPEDO containing INVITROGRO CP medium (1:9 (v/v). Then the cells were scraped and centrifuged at 1000*g* for 5 minutes at 4°C to collect the hepatocytes pellet. The pellet was dissolved in extraction buffer II and 2% SDS (1:1) for protein quantification by LC-MS/MS analyses.

SCH. About 0.35×10^6 hepatocytes/well were plated in a 24-well collagen-coated plate for 24 hours with 0.5 ml/well TORPEDO containing INVITROGRO CP medium (1:9 (v/v). Then the medium was replaced with TORPEDO containing INVITROGRO HI medium with 0.25 mg/ml matrigel. Medium was replaced daily with 0.5 ml/well fresh TORPEDO containing INVITROGRO HI. On day 4 of the sandwich culture, the cells were scraped and centrifuged at 1000*g* for 5 minutes at 4°C to collect the hepatocytes pellet. The pellet was dissolved in 2 ml extraction buffer II and 2% SDS (1:1) for protein quantification by LC-MS/MS analyses.

Plasma Membrane Isolation from Suspended, Plated, and Sandwich-Cultured Human Hepatocytes by Cell Surface Biotinylation

Plasma membrane from SH, PH, and SCH was isolated, using a cell surface biotinylation methodology optimized in our laboratory (Kumar et al., 2017, 2018). The cell surface biotinylation method nonspecifically biotinylates plasma membrane proteins, including many proteins other than the transporters of interest. This nonspecific biotinylation allows one to isolate pure plasma membrane fractions from cells and hepatocytes. Briefly, SH ($\sim 8.4 \times 10^6$ hepatocytes) or PH/SCH (0.35×10^6 hepatocytes/well, 24-well plate) were incubated with 10 ml or 0.5 ml/well sulfosuccinimidyl-2-(biotinamido) ethyl-1, 3-dithiopropionate (0.78 mg/ml), respectively, at 37°C for 30 minutes. Then hepatocytes were washed twice with 10 ml phosphate-buffered saline buffer, scraped, and centrifuged at 500*g* for 3 minutes at 4°C to collect the hepatocytes pellet and lysed in 750 μl lysis buffer. After cell lysis, the biotinylated plasma membrane was isolated using neutravidin resin columns. Fractions representing biotinylated (plasma membrane fraction) and nonbiotinylated (intracellular fraction) were collected for protein quantification by LC-MS/MS analyses. As a quality control check, only samples that fell within the range of 100% $\pm$ 30% recovery of cellular proteins (relative to the homogenate) were deemed acceptable.

Applying the cell surface biotinylation method (Kumar et al., 2017) to SCH posed an interesting question. Should this method be applied to SCH in the presence or absence of calcium (Ca^{2+})? In the presence of Ca^{2+}, the hepatocytes form tight junctions (Pfeifer et al., 2013). These tight junctions, which may hinder accessibility of the biotinylation reagent to the canalicular membrane, are disrupted in the absence of Ca^{2+}. Therefore, to investigate whether there was any difference in the efficiency of cell surface biotinylation, we conducted a pilot study of cell surface biotinylation of SCH in the presence and absence of Ca^{2+}. The abundance of plasma membrane hepatic transporters as a percentage of total (homogenate), in presence or absence of Ca^{2+}, was statistically not different (Wilcoxon signed rank test; Supplemental Fig. 1). Therefore, all subsequent cell surface biotinylation experiments in hepatocytes were conducted in the presence of Ca^{2+}.

LC-MS/MS Quantification of Total and Plasma Membrane Transporter Abundance

Total protein content (wt/wt) in human liver and hepatocytes homogenate was quantified by the bicinchoninic acid assay. Transporter abundance was quantified using validated and optimized proteomics protocols implemented in our laboratory (Prasad and Unadkat, 2014a,b; Wang et al., 2015). Briefly, liver tissue/hepatocyte homogenates (equivalent to 0.2 mg total protein) were treated with 45 μl ammonium bicarbonate buffer (100 mM, pH 7.8), 25 μl 3% sodium deoxycholate (w/v), 12.5 μl DTT (250 mM), and 5 μl human albumin (10 mg/ml). Proteins present in the sample were denatured, and disulfide bond between cysteine residues was reduced by incubation at 95°C for 5 minutes, followed by the addition of 25 μl iodoacetamide (200 mM; an alkylating agent) and treatment with ice-cold methanol (0.5 ml), chloroform (0.2 ml), and water (0.45 ml) and centrifugation (12,000*g*). Lastly, the protein sample was digested with 20 μl trypsin (equivalent to 3.2 μg trypsin), mixed with 20 μl labeled internal standards, and followed by centrifugation at 5000*g* for 5 minutes at 4°C, and 5 μl supernatant was introduced into the LC-MS/MS system. The calibration standards were prepared by spiking peptide standards into the extraction buffer II of the membrane protein extraction kit. As an internal biologic control, total membrane isolated from 39 human livers was pooled (PHL) (Wang et al., 2016), aliquoted, and stored at −80°C. This PHL sample was processed and analyzed in each

LC-MS/MS run to ensure that the data from PHL were consistent (within 100% ± 20%) with the liver transporter abundance data published by us (Wang et al., 2016). We note in this work that the surrogate peptide of interest for each transporter protein was localized intracellularly (except NTCP; Supplemental Table 3). Thus, it will not be modified by the biotinylation reagent (because this reagent does not permeate the cell membrane) (Supplemental Fig. 3).

Samples were analyzed, as described before (Kumar et al., 2018). Briefly, AB Sciex 6500 triple-quadrupole mass spectrometer (Sciex, Framingham, MA) coupled to the Water Acquity Ultra-Performance Liquid Chromatography (UPLC) system (Waters, Milford, MA) was operated in electrospray positive ionization mode for LC-MS/MS analysis of the signature peptides (Supplemental Table 2). The NTCP peptide was quantified on a Waters Xevo TQS tandem mass spectrometer (Supplemental Table 2) due to the greater sensitivity of detection of this peptide afforded by this instrument. The transitions from doubly charged parent ion to singly charged product ions for the analyte peptides and their respective stable isotope-labeled peptides were monitored (Supplemental Table 2). The chromatographic separation and resolution were obtained on an Acquity UPLC HSS T3 column (1.8 μm, 2.1 × 100 mm) with a 0.2-μm inlet frits (Waters). Mobile phases (0.3 ml/min) consisted of 0.1% formic acid in water (A) and 0.1% formic acid in acetonitrile (B). The gradient program for UPLC method for determination of transporters in hepatocytes and LT was as follows: 0–3 minutes, 3% B; 3–10 minutes, 3%–13% B; 10–20 minutes, 13%–25% B; 20–22 minutes, 25%–33.3% B; 22–24 minutes, 33.3%–80% B; 24–25 minutes, 80% B; 25–26 minutes, 80%–3% B; 26–30 minutes, 3% B, including washing and re-equilibration for 4 minutes.

In all of the above analyses, Na^+-K^+ ATPase and calreticulin were used as positive controls of plasma membrane and intracellular (endoplasmic reticulum) marker proteins, respectively. For calreticulin, the stable labeled internal standard was not procured; therefore, the stable labeled internal standard of Na^+-K^+-ATPase was used to estimate the calreticulin peak area ratio, as reported previously (Kumar et al., 2017, 2018). The unlabeled peptide of Na^+-K^+ ATPase was not procured. Thus, Na^+-K^+ ATPase area ratio was used to determine the correlation with hepatic transporter abundance in LT and hepatocyte models (Supplemental Fig. 2).

Data and Statistical Analyses

Determination of Total Transporter Abundance in LT and Hepatocyte Models. For each donor, the total transporter abundance in the homogenates of LT and hepatocyte models was determined as a mean ± S.D. of three to five independent experiments (only single experiment for NTCP).

Determination of Percentage of PMA of Transporters in Hepatocyte Models. The percentage of PMA of hepatic transporters, calreticulin, and Na^+-K^+ ATPase in hepatocyte models (using cell surface biotinylation) was calculated, as reported previously (Kumar et al., 2017). The PMA of transporters in hepatocyte models was obtained by multiplying the percentage of PMA with the total transporter abundance in homogenate, and the data are reported as mean ± S.D. of four lots of hepatocytes from three independent experiments (only single experiment for NTCP).

Statistical Analysis. Friedman test with Dunn's multiple comparison non-parametric statistical method (using Prism 7, version 7.03) was used to compare (pairwise comparison for each donor) the percentage of PMA, PMA or total abundance of the hepatic transporters in hepatocyte models, and LT. Wilcoxon signed rank test was used to compare the percentage of PMA of hepatic transporters in SCH in the presence or absence of calcium.

Results

A Comparison of Total Transporter Abundance in Suspended, Plated, Sandwich-Cultured Human Hepatocytes and Human Liver Tissue. In general, the total transporter abundance was most variable between the donors and between SCH and other hepatocyte models or LT. For each donor, the total abundance of sinusoidal uptake transporter proteins (OATP1B1/2B1/1B3, OCT1, and OAT2) was relatively consistent between different hepatocyte models and LT (Fig. 1). However, the total protein abundance of the sinusoidal efflux transporter, MRP3, and the canalicular efflux transporters, MRP2 and P-gp, was significantly increased in SCH compared with their respective LT (Fig. 1). NTCP and BSEP abundance in PH was significantly, but modestly, higher than LT, but similar to SH and SCH.

A Comparison of Plasma Membrane Abundance of Transporters in Suspended, Plated, and Sandwich-Cultured Human Hepatocytes. As expected, the localization of the intracellular (endoplasmic reticulum) marker, calreticulin, and the plasma membrane marker, Na^+-K^+ ATPase, was predominantly intracellular and in the plasma membrane, respectively (Fig. 2). For each donor, the percentage of PMA of hepatic transporters in the hepatocyte models was highly reproducible with % CV of <30%. The majority (i.e., >50%) of the sinusoidal uptake transporters were localized in the plasma membrane of the SH, PH, and SCH (Fig. 2). There was no significant difference in the percentage of PMA of sinusoidal uptake transporters in SH, PH, and SCH (except OATP1B1) (Fig. 2). Comparison of the PMA of NTCP in SCH versus other models could not be performed for YTW because NTCP could not be quantified in SCH for this donor (Fig. 3). The majority of the efflux transporters, P-gp (except in SCH) and BSEP, were intracellular, whereas the majority of MRP2 and MRP3 transporters were in the plasma membrane. The percentage of PMA of the efflux transporters, MRP2 and BSEP, was found to be similar in SH, PH, and SCH (Fig. 2). In contrast, the percentage of PMA of MRP3 and P-gp was significantly higher in SCH (69.3% and 57.5%) compared with SH (57.6% and 27.4%) (Fig. 2). The cell surface biotinylation method can be applied only to intact cells and not to tissues. Therefore, PMA of transporters was compared among only in the hepatocyte models. The abundance of sinusoidal uptake transporters in the plasma membrane in the different hepatocyte models was not significantly different (Fig. 3). In contrast, among the efflux transporters, only the PMA of MRP3, MRP2, and P-gp in SCH was found to be significantly greater than that in SH (Fig. 3). This difference was variable among the donors studied. For donor ADR, the change in PMA of MRP3, P-gp, and MRP2 between SCH versus SH was large, about 600%–2000%, whereas for JEL there was minimal or no change between SCH versus SH (Fig. 3).

Correlation of Total Transporter Abundance in Suspended, Plated, Sandwich-Cultured Human Hepatocytes, and Human Liver Tissue. The total abundance of the sinusoidal efflux, MRP3, and the canalicular efflux transporters, MRP2 and P-gp (but not BSEP), was highly correlated ($R^2 \geq 0.88$) with each other (Fig. 4, A–C). The total abundance of OATP1B1 and OATP2B1 showed good correlation with that of OAT2 and OCT1 (Fig. 4, D and E, $R^2 \geq 0.67$), respectively. The abundance of other transporters showed poor correlation ($R^2 \leq 0.5$) with each other (Fig. 4F; see Supplemental Table 3).

Correlation of Abundance of Total and Plasma Membrane Transporter with the Abundance of Na^+-K^+ ATPase in Suspended, Plated, and Sandwich-Cultured Human Hepatocytes. Total transporter abundance of sinusoidal and canalicular transporters showed poor correlation ($R^2 \leq 0.28$) with total abundance of Na^+-K^+ ATPase in the hepatocyte models (Supplemental Fig. 2A). Except for MRP2, MRP3, and P-gp, the same was true for PMA of these transporters. The PMA of MRP2, MRP3, and P-gp was highly correlated ($R^2 \geq 0.7$) with that of Na^+-K^+ ATPase (Supplemental Fig. 2B).

Discussion

To address the aims of our study, we deliberately incorporated, in our experiments, three distinct and unique design features, not hitherto implemented by others (Li et al., 2010; Jones et al., 2012; Schaefer et al., 2012; Vildhede et al., 2018). First, we systematically compared the changes in transporter abundance in SH, PH, and SCH relative to that in the liver tissue from which they were isolated. This design increased our power to discern the change in abundance of transporters in the hepatocyte models versus that in the corresponding liver tissue. Second, to avoid interbatch variability in total membrane yield, we determined the

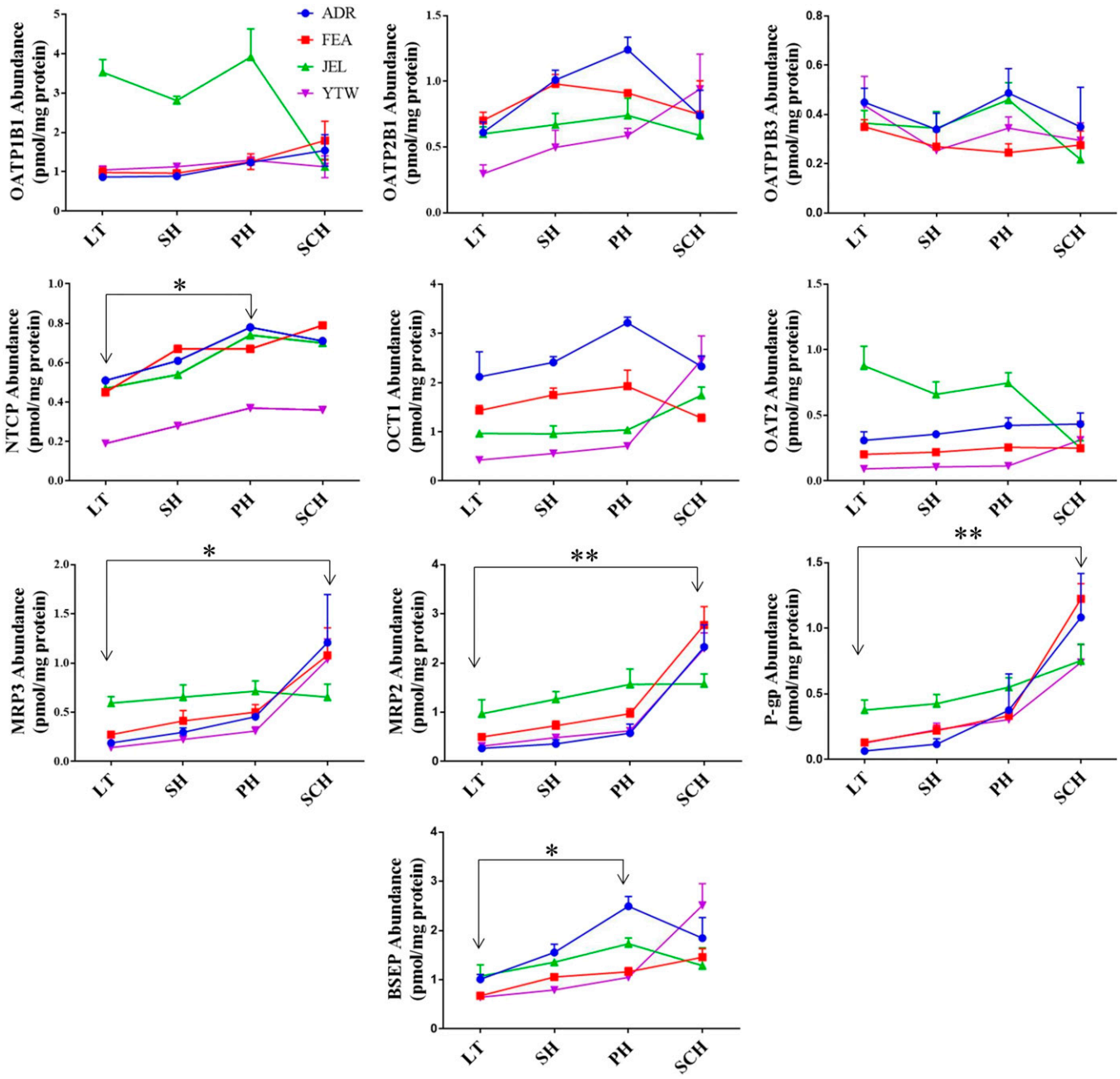

Fig. 1. Total hepatic transporter abundance in LT, SH, PH, and SCH. There was no significant difference in the total abundance of uptake transporters OATP1B1/2B1/1B3, OCT1, and OAT2 between LT, SH, PH, and SCH. In contrast, total abundance of the efflux transporters MRP2, MRP3, and P-gp was significantly greater in SCH vs. LT. NTCP and BSEP abundance was significantly higher in PH vs. LT. Data for each donor are mean ± S.D. of three to five independent experiments (only single experiment for NTCP). $*P < 0.05$; $**P < 0.01$.

transporter abundance in the homogenate rather than in the total membrane isolated from the various samples (Billington et al., 2018; Vildhede et al., 2018). However, the disadvantage of this design (Wegler et al., 2017) was that it did not allow us to quantify the low abundance transporters MATE1, MRP4, and BCRP. Third, because it is the transporter abundance in the plasma membrane that is functionally important for the uptake or efflux of drugs, we determined this abundance in the hepatocyte models used. The plasma membrane transporter abundance data also answered the question whether the change (if any) in plasma membrane transporter abundance in the hepatocyte models was due to the change in total abundance or the change in the percentage of PMA or both.

There was significant interindividual variability in total transporter abundance between hepatocyte donors. This interindividual variability in OATP1B1 abundance was not due to genetic polymorphisms (Supplemental Table 1), which are known to affect the transporter abundance/activity (Prasad et al., 2014; Li and Barton, 2018). We have shown that the hepatic abundance of OATP1B1 is haplotype-dependent and follows the order *1b (e.g., FEA and JEL) > *1a (e.g., YTW) > *5 (e.g., ADR) (Prasad et al., 2014). Despite having the same OATP1B1 haplotype as FEA, one donor, JEL (African American), demonstrated higher total abundance of OATP1B1 and behaved differently from the other donors with respect to total and PMA in SCH versus other hepatocyte models (Figs. 1 and 3).

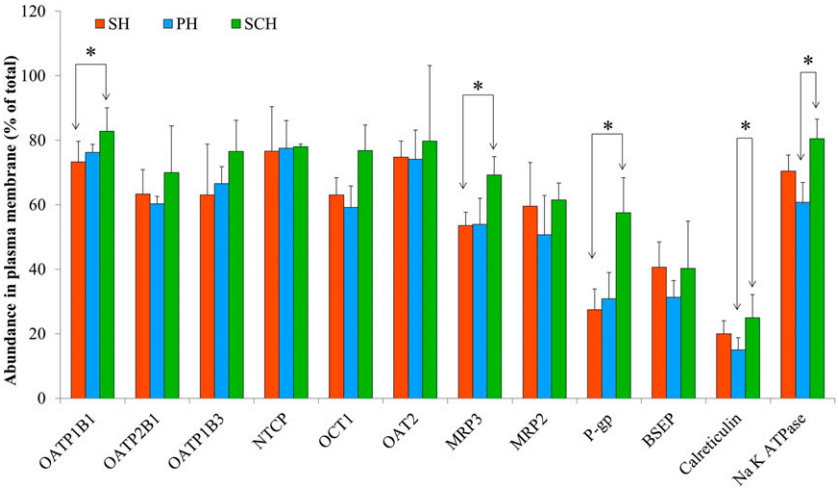

Fig. 2. Percentage of plasma membrane abundance of hepatic transporters in SH, PH, and SCH. Hepatic uptake transporters (OATP1B1/2B1/1B3, NTCP, OCT1, OAT2) were mostly (>50%) localized in the plasma membrane of SH, PH, or SCH. P-gp and BSEP were mostly localized intracellularly in SH and PH, but in SCH, the localization in the plasma membrane of P-gp, but not BSEP, increased significantly to >50%. Na^+-K^+ ATPase and calreticulin were used as a positive control for plasma membrane and intracellular (endoplasmic reticulum) marker, respectively. Cell surface biotinylation experiment was conducted in presence of calcium-containing Hanks' balanced salt solution buffer. Data are reported as mean ± S.D. of four hepatocyte donors (except SCH-NTCP: three donors), with data for each donor as the mean of three independent experiments (only single experiment for NTCP). $*P < 0.05$.

The lack of difference in the total abundance of the sinusoidal uptake transporters (except NTCP; Fig. 1) in the various hepatocyte models versus LT is contrary to our observation and those of others with rat hepatocytes. In the rat, a significant decrease in the total abundance of the sinusoidal Oatp transporters was observed in SCH versus LT (De Bruyn et al., 2013; Ishida et al., 2018). As was the case in this study for the suspended hepatocytes, we and others have previously shown that the total membrane abundance of MRP2, MRP3, P-gp, and BSEP (in total membrane) is similar between freshly isolated or cryopreserved hepatocytes versus human LT (Li et al., 2009b; Lundquist et al., 2014). The significantly higher total abundance of MRP2, MRP3, and P-gp in SCH versus LT (Fig. 1) is consistent with previously published data (although sparse) (Hoffmaster et al., 2004; Li et al., 2009a) obtained with Western blotting after cell lysis or quantitative proteomic analysis of total membrane (not homogenate) isolated from hepatocytes and LT. Similarly, rat Mrp2 abundance in cell lysate is stable in SCH over 4 days in culture (Zhang et al., 2005), but the abundance of rat P-gp, human P-gp, and MRP2 in cell lysate or total membrane isolated from SCH increases over 6 days in culture (Hoffmaster et al., 2004; Li et al., 2009a). Kimoto et al. (2012) have reported that OATP transporter abundance in human liver tissue is about twice that in cryopreserved human hepatocytes or SCH (Kimoto et al., 2012), but similar between cryopreserved human hepatocytes and SCH. Others have reported that all measured transporter abundance in total membrane was lower (except OCT1 and OAT2) in freshly isolated human hepatocytes compared with human liver tissue (Vildhede et al., 2015). However, the difference in transporter abundance between liver tissue and hepatocytes observed by others (Kimoto et al., 2012; Vildhede et al., 2015) could be due to differential loss in membrane as none of these studies was conducted with the homogenate of liver tissue or hepatocytes.

Because it is the PMA of the transporter that is important for in vitro to in vivo extrapolation (IVIVE) of transporter-mediated clearances, we determined the percentage of PMA in hepatocyte models. As indicated earlier, the cell surface biotinylation methodology used in this study to isolate plasma membrane cannot be applied to tissues; therefore, the percentage of PMA of transporters in LT could not be determined. Although most (>50%) of the uptake transporters were localized in the plasma membrane of the hepatocytes, so were some of the efflux transporters, namely MRP2 and MRP3. However, most of P-gp (except in SCH) and BSEP were localized in the intracellular compartment. When the hepatocytes were sandwich-cultured, the percentage of PMA of both MRP3 and P-gp increased significantly ($P < 0.05$) compared with that in the SH. This change was most remarkable for P-gp, in which the percentage of PMA of P-gp was ~twofold higher in SCH (~58%) than in SH or PH (~30%).

When the above data were combined, a clear picture emerged of the PMA of the transporters in the hepatocyte models. Although there was significant interindividual variability in the PMA of the transporters in SCH versus SH, the PMA in the other hepatocyte models (SH and PH) remained consistent with each other. Remarkably, PMA of MRP3, MRP2, and P-gp significantly increased in SCH versus SH with the greatest change occurring for P-gp (e.g., ~2000% in ADR). The increase in PMA of P-gp and MRP3 in SCH versus SH was due to an increase in total abundance (Fig. 1) as well as an increase in the percentage of PMA (Fig. 2). In contrast, the increased PMA of MRP2 in SCH versus SH was due to an increase in the total transporter abundance (Fig. 1) but not in the percentage of PMA (Fig. 2). This could be an alternate explanation for the widely reported internalization of MRP2 in SCH (see below).

There are contradictory reports about internalization or intracellular localization of canalicular efflux transporters, resulting in decreased abundance in the plasma membrane of hepatocyte models (SH and PH). In freshly isolated hepatocytes, rat Mrp2 and Mdr1a/b are predominately localized intracellularly (Bow et al., 2008). However, when sandwich-cultured (days 5 and 6), Mdr1a/b and MDR1 are predominantly expressed in the plasma membrane of rat and human hepatocytes, respectively (Hoffmaster et al., 2004). In contrast, immunolocalization studies of Lundquist et al. (2014) have shown that the majority of the ABC transporters (P-gp, MRP2, and BCRP) are localized in the plasma membrane of the cryopreserved human hepatocytes and human livers. They also demonstrated transport activity of BCRP and P-gp in plated human and rat hepatocytes, suggesting that some (or perhaps all) of these transporters are localized to the plasma membrane (Lundquist et al., 2014). Unfortunately, all of the localization studies cited above are immunolocalization studies. Thus, the percentage of transporters in the plasma membrane versus that in the intracellular compartments was not quantified. To our knowledge, ours is the first study to quantify PMA of hepatic transporters in SH, PH, and SCH. Nevertheless, our data, along with others (Hoffmaster et al., 2004; Lam and Benet, 2004; Lam et al., 2006; Bow et al., 2008; Lundquist et al., 2014), indicate that canalicular transporters in human suspended and plated hepatocytes are not all internalized, but are also present in the plasma membrane.

If the percentage of PMA of sinusoidal uptake transporters in SH is representative of the LT and all transporters expressed in the plasma membrane are functional, our data (Figs. 1–3) suggest that any of human hepatocyte models (SH or PH or SCH) can be used to predict the in vivo hepatic uptake clearance of drugs mediated by OATP1B1, OATP1B3,

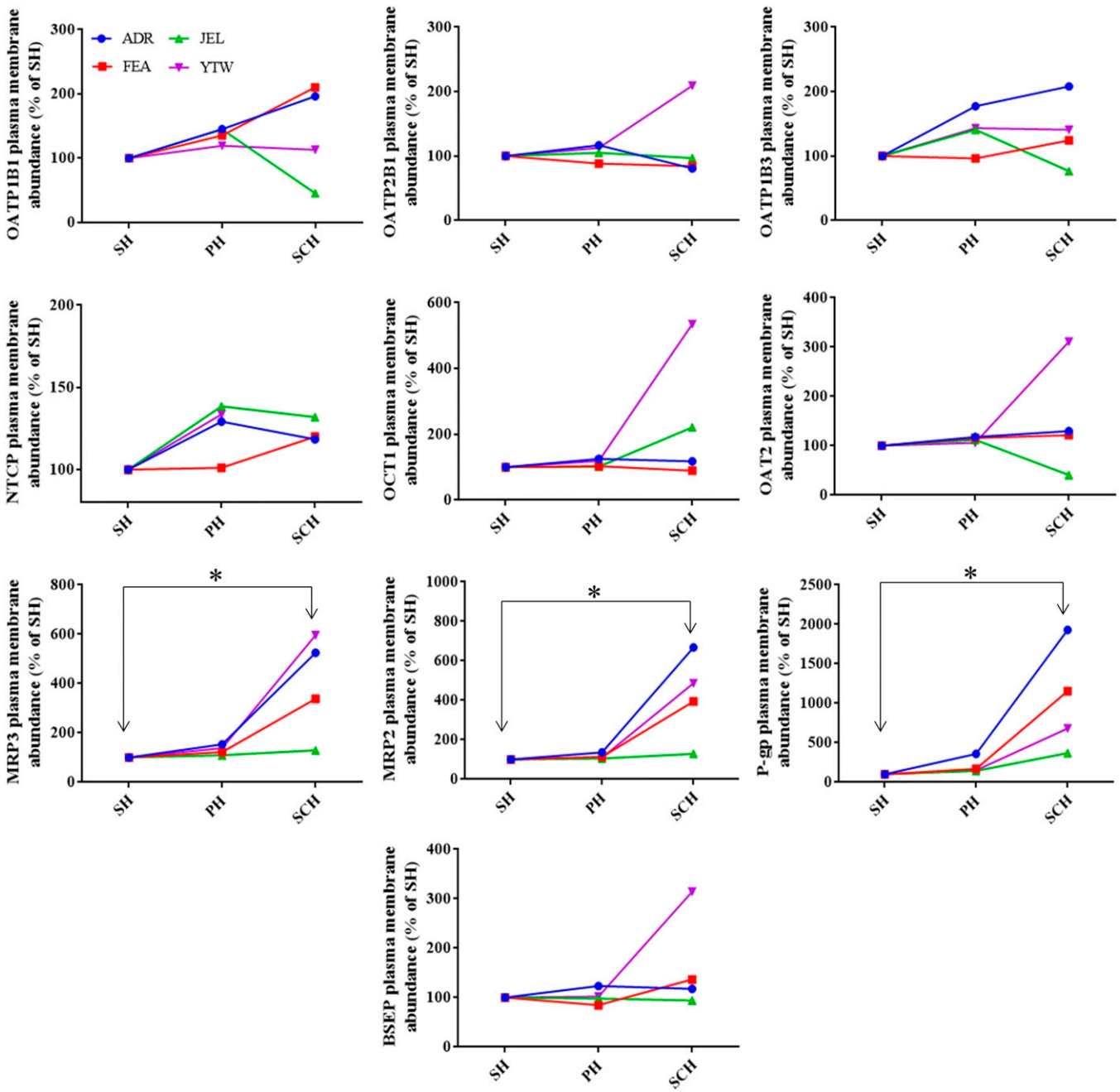

Fig. 3. Plasma membrane abundance of hepatic transporters in SH, PH, and SCH. Values are expressed as percentage of abundance relative to the respective SH (derived from Figs. 1 and 2). Of the transporters studied, the PMA of MRP2, MRP3, and P-gp was significantly higher in SCH vs. SH. Data for each donor are reported as mean of three to five independent experiments (only single experiment for NTCP). $*P < 0.05$.

OAT2, and OCT1 (Kumar et al., 2015) without the need to measure the plasma membrane or total abundance of the transporters. Likewise, SH or PH could be used to predict sinusoidal (or perhaps even biliary efflux) clearance of drugs without quantifying the total or PMA of these transporters. Whether SH or PH can be used to predict efflux clearance of drugs remains to be explored. In contrast, SCH, the most commonly used hepatocyte model to estimate in vivo CL_b, will overpredict CL_b and sinusoidal efflux clearance mediated by the transporters, MRP2/P-gp and MRP3, respectively, unless changes in the PMA of these transporters are quantified. It is worth noting that there are a few limitations to this conclusion. First, the PMA of the transporters in LT and the hepatocyte model is assumed to be proportional to their activity. Second, because there is considerable interindividual variability in the abundance of transporters, this conclusion is made based on a limited data set of four lots of hepatocytes. If the percentage of PMA of the transporter in LT is higher than in SH, PH, or SCH, then these hepatocyte models will underpredict the hepatic uptake clearances of drugs, but SCH will most likely overpredict efflux clearance (MRP2 or MRP3 or P-gp–mediated). Take, for example, MRP3, which shows the lowest increase (threefold) in total abundance in SCH versus LT. Thus, even if the percentage of PMA of MRP3 in LT is 100%, the SCH will overpredict the biliary clearance of drugs. If the percentage of PMA of MRP3 in LT is much less than in SH, this overprediction will be even greater.

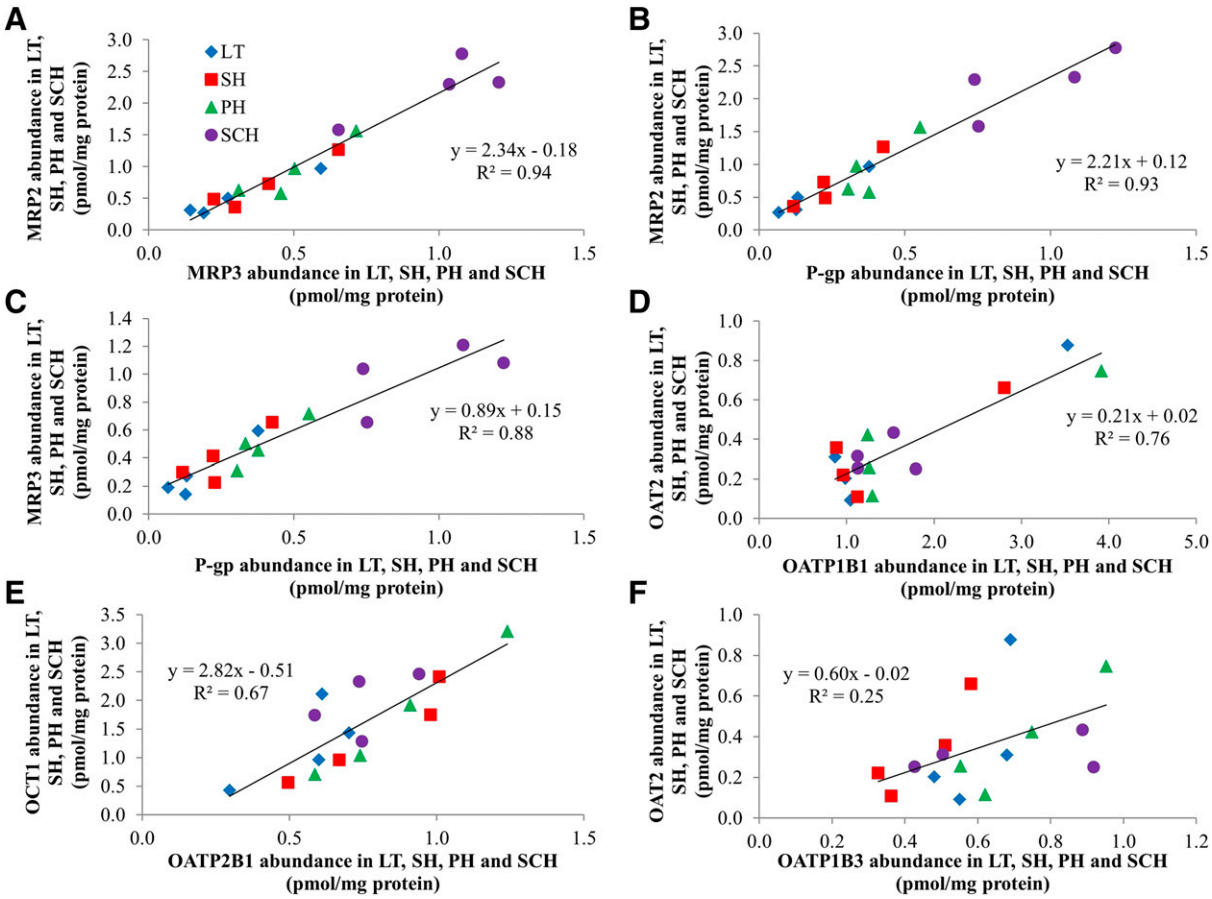

Fig. 4. Correlation of total transporter abundance across LT, SH, PH, and SCH. The total abundance of MRP2, MRP3, and P-gp was highly correlated with each other [(A–C), $R^2 \geq 0.88$]. OAT2 and OCT1 abundance showed good correlation with OATP1B1 and OATP2B1 [(D and E), $R^2 \geq 0.67$], respectively, but the abundance of OAT2 was poorly correlated ($R^2 \leq 0.5$) with OATP1B3 [(F); representative of those showing poor correlation—see Supplemental Table 3]. Each datum is mean of three to five independent experiments.

The high correlation ($R^2 > 0.67$) of total transporter abundance of MRP2 versus MRP3, MRP2 versus P-gp, MRP3 versus P-gp, OAT2 versus OATP1B1, and OCT1 versus OATP2B1 (Fig. 4) suggests a common regulatory mechanism of these transporters (Chen et al., 2012). The good correlation of plasma membrane canalicular efflux transporter (MRP2, MRP3, and P-gp) abundance with Na^+-K^+ ATPase (Supplemental Fig. 2B) could be the result of simultaneous targeting of these proteins to the newly formed canalicular membrane in SCH.

In summary, we have conducted a systematic study to quantify the total and PMA of hepatic transporters in commonly used human hepatocyte models and compared it with total abundance of the transporters in LT from which they were derived. Based on the total abundance data, all three hepatocyte models, suspended, plated, and sandwich-cultured human hepatocytes, can be used for IVIVE sinusoidal uptake clearance of drugs in humans. However, for IVIVE of efflux clearance, although all three models could potentially be used, the increase in PMA of MRP3, MPR2, and P-gp in SCH needs to be considered. Of course, for both approaches, the complementary in vitro clearance of the drug by the respective transporter needs to be obtained. As to whether such data can be reliably obtained for the efflux transporters (in SH and PH) needs to be explored. Importantly, these data do not support the hypothesis that lower abundance of transporters (total or plasma membrane) in the hepatocyte models versus LT is the reason for lack of success in IVIVE of transporter-mediated hepatobiliary clearance of drugs in humans. Thus, other factors to explain this failure (if any) need to be sought. Such factors include correct identification of the rate-determining step in the clearance of the drug, considering the difference between in vitro and in vivo in the mechanism of transport of the drug (Kumar et al., 2018), and refining in vitro methods to accurately determine both the active and passive clearance of the drug. We have recently shown that when these factors are carefully considered, the in vivo hepatic and renal uptake clearance of rosuvastatin and metformin can be accurately predicted by proteomics-informed scaling of the in vitro uptake clearance of these drugs in transporter-expressing cells (Ishida et al., 2018; Kumar et al., 2018). Such studies with additional drugs, including prediction(s) and verification (e.g., by positron emission tomography imaging) of in vivo efflux clearance using this proteomics-informed approach, are needed.

Acknowledgments

We thank Tot Bui Nguyen for support in cell surface biotinylation experiments and LC-MS/MS proteomics.

Authorship Contributions

Participated in research design: Kumar, Salphati, Hop, Xiao, Lai, Mathias, Chu, Humphreys, Liao, Heyward, Unadkat.

Conducted experiments: Kumar.

Contributed new reagents or analytic tools: Heyward.

Performed data analysis: Kumar, Unadkat.

Wrote or contributed to the writing of the manuscript: Kumar, Salphati, Hop, Xiao, Lai, Mathias, Chu, Humphreys, Liao, Heyward, Unadkat.

References

Abe K, Bridges AS, Yue W, and Brouwer KL (2008) In vitro biliary clearance of angiotensin II receptor blockers and 3-hydroxy-3-methylglutaryl-coenzyme A reductase inhibitors in sandwich-cultured rat hepatocytes: comparison with in vivo biliary clearance. *J Pharmacol Exp Ther* **326**:983–990.

Billington S, Ray AS, Salphati L, Xiao G, Chu X, Humphreys WG, Liao M, Lee CA, Mathias A, Hop CECA, et al. (2018) Transporter expression in noncancerous and cancerous liver tissue from donors with hepatocellular carcinoma and chronic hepatitis C infection quantified by LC-MS/MS proteomics. *Drug Metab Dispos* **46**:189–196.

Bow DA, Perry JL, Miller DS, Pritchard JB, and Brouwer KL (2008) Localization of P-gp (Abcb1) and Mrp2 (Abcc2) in freshly isolated rat hepatocytes. *Drug Metab Dispos* **36**:198–202.

Chen Y, Tang Y, Guo C, Wang J, Boral D, and Nie D (2012) Nuclear receptors in the multidrug resistance through the regulation of drug-metabolizing enzymes and drug transporters. *Biochem Pharmacol* **83**:1112–1126.

De Bruyn T, Chatterjee S, Fattah S, Keemink J, Nicolaï J, Augustijns P, and Annaert P (2013) Sandwich-cultured hepatocytes: utility for in vitro exploration of hepatobiliary drug disposition and drug-induced hepatotoxicity. *Expert Opin Drug Metab Toxicol* **9**:589–616.

Hoffmaster KA, Turncliff RZ, LeCluyse EL, Kim RB, Meier PJ, and Brouwer KL (2004) P-glycoprotein expression, localization, and function in sandwich-cultured primary rat and human hepatocytes: relevance to the hepatobiliary disposition of a model opioid peptide. *Pharm Res* **21**:1294–1302.

Ishida K, Ullah M, Tóth B, Juhasz V, and Unadkat JD (2018) Successful prediction of in vivo hepatobiliary clearances and hepatic concentrations of rosuvastatin using sandwich-cultured rat hepatocytes, transporter-expressing cell lines, and quantitative proteomics. *Drug Metab Dispos* **46**:66–74.

Jones HM, Barton HA, Lai Y, Bi YA, Kimoto E, Kempshall S, Tate SC, El-Kattan A, Houston JB, Galetin A, et al. (2012) Mechanistic pharmacokinetic modeling for the prediction of transporter-mediated disposition in humans from sandwich culture human hepatocyte data. *Drug Metab Dispos* **40**:1007–1017.

Kimoto E, Yoshida K, Balogh LM, Bi YA, Maeda K, El-Kattan A, Sugiyama Y, and Lai Y (2012) Characterization of organic anion transporting polypeptide (OATP) expression and its functional contribution to the uptake of substrates in human hepatocytes. *Mol Pharm* **9**:3535–3542.

Kumar V, Nguyen TB, Tóth B, Juhasz V, and Unadkat JD (2017) Optimization and application of a biotinylation method for quantification of plasma membrane expression of transporters in cells. *AAPS J* **19**:1377–1386.

Kumar V, Prasad B, Patilea G, Gupta A, Salphati L, Evers R, Hop CE, and Unadkat JD (2015) Quantitative transporter proteomics by liquid chromatography with tandem mass spectrometry: addressing methodologic issues of plasma membrane isolation and expression-activity relationship. *Drug Metab Dispos* **43**:284–288.

Kumar V, Yin J, Billington S, Prasad B, Brown CDA, Wang J, and Unadkat JD (2018) The importance of incorporating OCT2 plasma membrane expression and membrane potential in IVIVE of metformin renal secretory clearance. *Drug Metab Dispos* **46**:1441–1445.

Lam JL and Benet LZ (2004) Hepatic microsome studies are insufficient to characterize in vivo hepatic metabolic clearance and metabolic drug-drug interactions: studies of digoxin metabolism in primary rat hepatocytes versus microsomes. *Drug Metab Dispos* **32**:1311–1316.

Lam JL, Okochi H, Huang Y, and Benet LZ (2006) In vitro and in vivo correlation of hepatic transporter effects on erythromycin metabolism: characterizing the importance of transporter-enzyme interplay. *Drug Metab Dispos* **34**:1336–1344.

Li N, Bi YA, Duignan DB, and Lai Y (2009a) Quantitative expression profile of hepatobiliary transporters in sandwich cultured rat and human hepatocytes. *Mol Pharm* **6**:1180–1189.

Li N, Singh P, Mandrell KM, and Lai Y (2010) Improved extrapolation of hepatobiliary clearance from in vitro sandwich cultured rat hepatocytes through absolute quantification of hepatobiliary transporters. *Mol Pharm* **7**:630–641.

Li N, Zhang Y, Hua F, and Lai Y (2009b) Absolute difference of hepatobiliary transporter multidrug resistance-associated protein (MRP2/Mrp2) in liver tissues and isolated hepatocytes from rat, dog, monkey, and human. *Drug Metab Dispos* **37**:66–73.

Li R and Barton HA (2018) Explaining ethnic variability of transporter substrate pharmacokinetics in healthy Asian and Caucasian subjects with allele frequencies of OATP1B1 and BCRP: a mechanistic modeling analysis. *Clin Pharmacokinet* **57**:491–503.

Lundquist P, Englund G, Skogastierna C, Lööf J, Johansson J, Hoogstraate J, Afzelius L, and Andersson TB (2014) Functional ATP-binding cassette drug efflux transporters in isolated human and rat hepatocytes significantly affect assessment of drug disposition. *Drug Metab Dispos* **42**:448–458.

Naritomi Y, Terashita S, Kagayama A, and Sugiyama Y (2003) Utility of hepatocytes in predicting drug metabolism: comparison of hepatic intrinsic clearance in rats and humans in vivo and in vitro. *Drug Metab Dispos* **31**:580–588.

Pfeifer ND, Yang K, and Brouwer KL (2013) Hepatic basolateral efflux contributes significantly to rosuvastatin disposition I: characterization of basolateral versus biliary clearance using a novel protocol in sandwich-cultured hepatocytes. *J Pharmacol Exp Ther* **347**:727–736.

Prasad B, Evers R, Gupta A, Hop CE, Salphati L, Shukla S, Ambudkar SV, and Unadkat JD (2014) Interindividual variability in hepatic organic anion-transporting polypeptides and P-glycoprotein (ABCB1) protein expression: quantification by liquid chromatography tandem mass spectroscopy and influence of genotype, age, and sex. *Drug Metab Dispos* **42**:78–88.

Prasad B and Unadkat JD (2014a) Comparison of heavy labeled (SIL) peptide versus SILAC protein internal standards for LC-MS/MS quantification of hepatic drug transporters. *Int J Proteomics* **2014**:451510.

Prasad B and Unadkat JD (2014b) Optimized approaches for quantification of drug transporters in tissues and cells by MRM proteomics. *AAPS J* **16**:634–648.

Schaefer O, Ohtsuki S, Kawakami H, Inoue T, Liehner S, Saito A, Sakamoto A, Ishiguro N, Matsumaru T, Terasaki T, et al. (2012) Absolute quantification and differential expression of drug transporters, cytochrome P450 enzymes, and UDP-glucuronosyltransferases in cultured primary human hepatocytes. *Drug Metab Dispos* **40**:93–103.

Soars MG, McGinnity DF, Grime K, and Riley RJ (2007) The pivotal role of hepatocytes in drug discovery. *Chem Biol Interact* **168**:2–15.

Vildhede A, Kimoto E, Rodrigues AD, and Varma MVS (2018) Quantification of hepatic organic anion transport proteins OAT2 and OAT7 in human liver tissue and primary hepatocytes. *Mol Pharm* **15**:3227–3235.

Vildhede A, Wiśniewski JR, Norén A, Karlgren M, and Artursson P (2015) Comparative proteomic analysis of human liver tissue and isolated hepatocytes with a focus on proteins determining drug exposure. *J Proteome Res* **14**:3305–3314.

Wang L, Collins C, Kelly EJ, Chu X, Ray AS, Salphati L, Xiao G, Lee C, Lai Y, Liao M, et al. (2016) Transporter expression in liver tissue from subjects with alcoholic or hepatitis C cirrhosis quantified by targeted quantitative proteomics. *Drug Metab Dispos* **44**:1752–1758.

Wang L, Prasad B, Salphati L, Chu X, Gupta A, Hop CE, Evers R, and Unadkat JD (2015) Interspecies variability in expression of hepatobiliary transporters across human, dog, monkey, and rat as determined by quantitative proteomics. *Drug Metab Dispos* **43**:367–374.

Wegler C, Gaugaz FZ, Andersson TB, Wiśniewski JR, Busch D, Gröer C, Oswald S, Norén A, Weiss F, Hammer HS, et al. (2017) Variability in mass spectrometry-based quantification of clinically relevant drug transporters and drug metabolizing enzymes. *Mol Pharm* **14**:3142–3151.

Zhang P, Tian X, Chandra P, and Brouwer KL (2005) Role of glycosylation in trafficking of Mrp2 in sandwich-cultured rat hepatocytes. *Mol Pharmacol* **67**:1334–1341.

Zou P, Liu X, Wong S, Feng MR, and Liederer BM (2013) Comparison of in vitro-in vivo extrapolation of biliary clearance using an empirical scaling factor versus transport-based scaling factors in sandwich-cultured rat hepatocytes. *J Pharm Sci* **102**:2837–2850.

Address correspondence to: Dr. Jashvant D. Unadkat, Department of Pharmaceutics, P.O. Box 357610, University of Washington, Seattle, WA 98195. E-mail: jash@uw.edu

SUPPLEMENTAL INFORMATION

A Comparison of Total and Plasma Membrane Abundance of Transporters in Suspended, Plated, Sandwich-Cultured Human Hepatocytes *vs.* Human Liver Tissue Using Quantitative Targeted Proteomics and Cell-Surface Biotinylation

Vineet Kumar, Laurent Salphati, Cornelis E. C. A. Hop, Guangqing Xiao, Yurong Lai, Anita Mathias, Xiaoyan Chu, W. Griffith Humphreys, Mingxiang Liao, Scott Heyward and Jashvant D. Unadkat

Department of Pharmaceutics, University of Washington, Seattle, Washington (VK and JDU)

Drug Metabolism and Pharmacokinetics, Genentech, Inc., South San Francisco, California (LS and CECAH)

DMPK, Biogen Idec, Cambridge, Massachusetts (GX[#])

 # Present address: Takeda Pharmaceuticals International Co., Cambridge, Massachusetts

Departments of Clinical Research, Clinical Pharmacology, and Drug Metabolism and Pharmacokinetics, Gilead Sciences, Inc., Foster City, California (YL and AM)

Pharmacokinetics, Pharmacodynamics and Drug Metabolism, Merck & Co., Rahway, New Jersey (XC)

Bristol-Myers Squibb Company, Princeton, New Jersey (WGH[*])

** Present address: Aranmore Pharma Consultant, Trenton, New Jersey*

Takeda Pharmaceuticals International Co., Cambridge, Massachusetts (ML[$])

$ Present address: Clovis Oncology, San Francisco, California

BioIVT, Baltimore, Maryland (SH)

Journal: Drug metabolism and disposition

The material includes three supplemental Figures and four supplemental Tables.

Supplemental Fig. 1. Percent plasma membrane abundance of hepatic transporters, calreticulin and Na^+-K^+ ATPase in SCH in the presence and absence of calcium. The percent PMA of hepatic transporters in the presence and absence of calcium was not significantly different (Wilcoxon signed rank test). The percent PMA of the transporters was consistent with the data shown in Fig. 2. Na^+-K^+ ATPase and calreticulin were used as a positive control as plasma membrane and intracellular (endoplasmic reticulum) markers respectively. Data are mean±SD of 4 hepatocyte donors.

Supplemental Fig. 2. Correlation of Total (A) and plasma membrane (B) transporter and Na^+-K^+ ATPase abundance in SH, PH and SCH. Of the transported studied, total abundance of the transporter was poorly correlated ($R^2 \leq 0.28$) with total abundance of Na^+-K^+ ATPase (A). Only PMA of MRP2, MRP3, and P-gp was highly correlated ($R^2 \geq 0.7$) with the PMA of Na^+-K^+ ATPase (B). The latter is shown as an area ratio (ratio of the Na^+-K^+ ATPase analyte peptide peak and Na^+-K^+ ATPase labeled internal standard peptide peak) because we did not have the standards of the analyte peptide (see methods). Each datum is mean of 3-5 independent experiments.

Supplemental Fig. 3. A schematic diagram of the biotinylation of plasma membrane proteins in hepatocyte models and transporter-expressing cells. Cell surface biotinylation reagent (Sulfo-NHS-SS-Biotin) reacts non-specifically with free primary amines of plasma membrane proteins. The ability of this biotinylation reagent to permeate the plasma membrane and biotinylate the intracellular peptide of interest is limited due to its polarity.

Supplemental Table 1. Demographic information and genotype of OATP1B1 of the hepatocyte donors

Lot #	Age	BMI	Gender	Race	Alcohol/ Tobacco/ Substance use	OATP1B1 Haplotype	OATP1B1 (SLCO1B1)		
							A388G	T521C	G1463C
ADR	38	28.7	Female	Caucasian	No	*5	A/A	T/C	G/C
FEA	57	32.4	Female	Caucasian	No	*1b	A/G	T/T	G/C
JEL	27	28.2	Female	African American	No	*1b	A/G	T/T	G/C
YTW	19	18.8	Male	Caucasian	No	*1a	G/G	T/T	G/C

Supplemental Table 2. MRM parameters of peptides selected for targeted analysis of human hepatic transporter abundance. The labeled amino acid residue of the internal standard is shown in bold.

AB Sciex 6500 triple-quadrupole mass spectrometer parameters					
Protein	Surrogate Peptide	Parent ion (m/z)	Product ion (m/z)	Declustering potential (V)	Collision energy (V)
OATP1B1	NVTGFFQSFK	587.9	961.4	50	24
	NVTGFFQSF**K**	591.9	969.5		
OATP2B1	VLAVTDSPAR	514.8	816.4	60	26
	VLAVTDSPA**R**	519.8	826.4		
OATP1B3	NVTGFFQSLK	570.8	927.5	60	23
	NVTGFFQSL**K**	574.8	935.5		
OCT1	LSPSFADLFR	576.8	476.7	60	27
	LSPSFADLF**R**	581.8	481.8		
OAT2	NVALLALPR	483.8	753.5	56.4	19.3
	NVALLALP**R**	488.8	763.5		
MRP3	ADGALTQEEK	531.3	747.4	60	26
	ADGALTQEE**K**	535.3	755.4		
MRP2	LTIIPQDPILFSGSLR	885.4	665.5	60	39
	LTIIPQDPILFSGSL**R**	890.5	670.4		
P-gp	NTTGALTTR	467.8	719.4	70	26
	NTTGALTT**R**	472.8	729.4		
BSEP	STALQLIQR	515.3	657.4	68.7	22.4
	STALQLIQ**R**	520.3	667.4		
Na^+-K^+ ATPase	AAVPDAVGK	414.2	586.3	61.3	18.8
	AAVPDAVG**K**	418.2	594.3		
Calreticulin	EQFLDGDGWTSR	705.8	893.4	50	33
Waters Xevo TQS tandem mass spectrometer parameters					
Protein	Surrogate Peptide	Parent ion (m/z)	Product ion (m/z)	Cone voltage (V)	Collision energy (V)
NTCP	GIYDGDLK	440.7	710.1	30	10
	GIYDGDL**K**	444.7	718.3		
Na^+-K^+ ATPase	AAVPDAVGK	414.2	586.3	30	14
	AAVPDAVG**K**	418.2	594.3		
Calreticulin	EQFLDGDGWTSR	705.8	893.4	35	18

Supplemental Table 3. Correlation (R^2) of total transporter abundance across LT, SH, PH, and SCH. Transporters showing good correlation ($R^2 \geq 0.67$) in their total abundance are in bold.

	OATP1B1	***OATP2B1***	***OATP1B3***	***NTCP***	***OCT1***	***OAT2***	***MRP3***	***MRP2***	***P-gp***	***BSEP***
OATP1B1	1									
OATP2B1	0.017	1								
OATP1B3	0.299	0.005	1							
NTCP	0.044	0.379	0.227	1						
OCT1	0.130	**0.671**	0.010	0.288	1					
OAT2	**0.762**	0.024	0.245	0.117	0.002	1				
MRP3	0.112	0.055	0.283	0.234	0.072	0.126	1			
MRP2	0.086	0.013	0.244	0.182	0.018	0.050	**0.938**	1		
P-gp	0.054	0.008	0.301	0.243	0.024	0.027	**0.878**	**0.927**	1	
BSEP	0.013	0.494	0.159	0.214	0.510	0.109	0.386	0.266	0.246	1

Supplemental Table 4. Topology of selected unique peptides[#]. All selected peptides are localized in the intracellular domain (except OAT2 and NTCP) and are not exposed to the biotinylation reagent present in the extracellular space.

Protein	Peptide	Amino acid sequence in protein[#]	Localization[#]
OATP1B1	NVTGFFQSFK	321-330	Intracellular
OATP2B1	VLAVTDSPAR	314-323	Intracellular
OATP1B3	NVTGFFQSLK	321-330	Intracellular
NTCP	GIYDGDLK	144-151	Extracellular[$]
OCT1	LSPSFADLFR	330-330	Intracellular
OAT2	NVALLALPR	20-28	Intracellular and transmembrane[*]
MRP3	ADGALTQEEK	939-948	Intracellular
MRP2	LTIIPQDPILFSGSLR	1377-1392	Intracellular
P-gp	NTTGALTTR	809-817	Intracellular
BSEP	STALQLIQR	461-470	Intracellular
Na^+-K^+ ATPase	AAVPDAVGK	587-595	Intracellular
Calreticulin	EQFLDGDGWTSR	25-36	ER lumen

Reference: https://www.uniprot.org, $: http://topcons.cbr.su.se/pred/result/rst_1STpul/

*****Amino acid "N" (Asparagine, number 20) is localized intracellularly and the rest of the amino acids (VALLALPR, number 21-28) are localized in the transmembrane domain.

Supplemental Fig. 1.

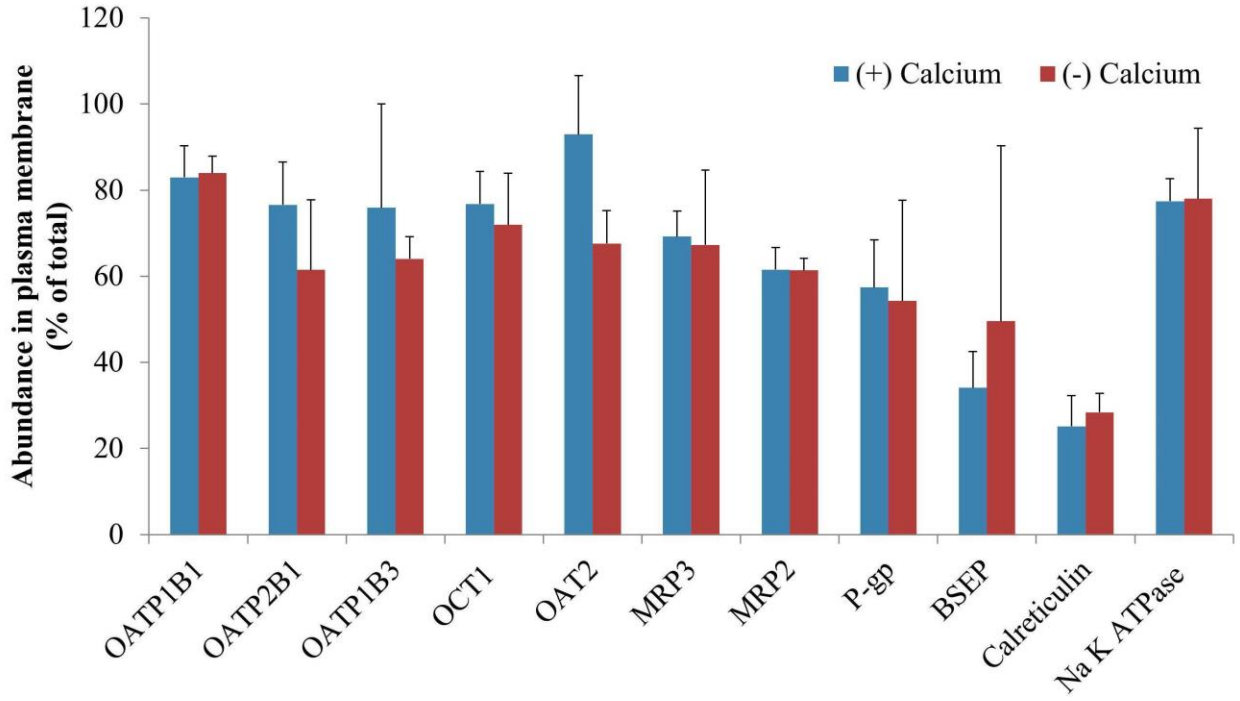

Supplemental Fig. 2.

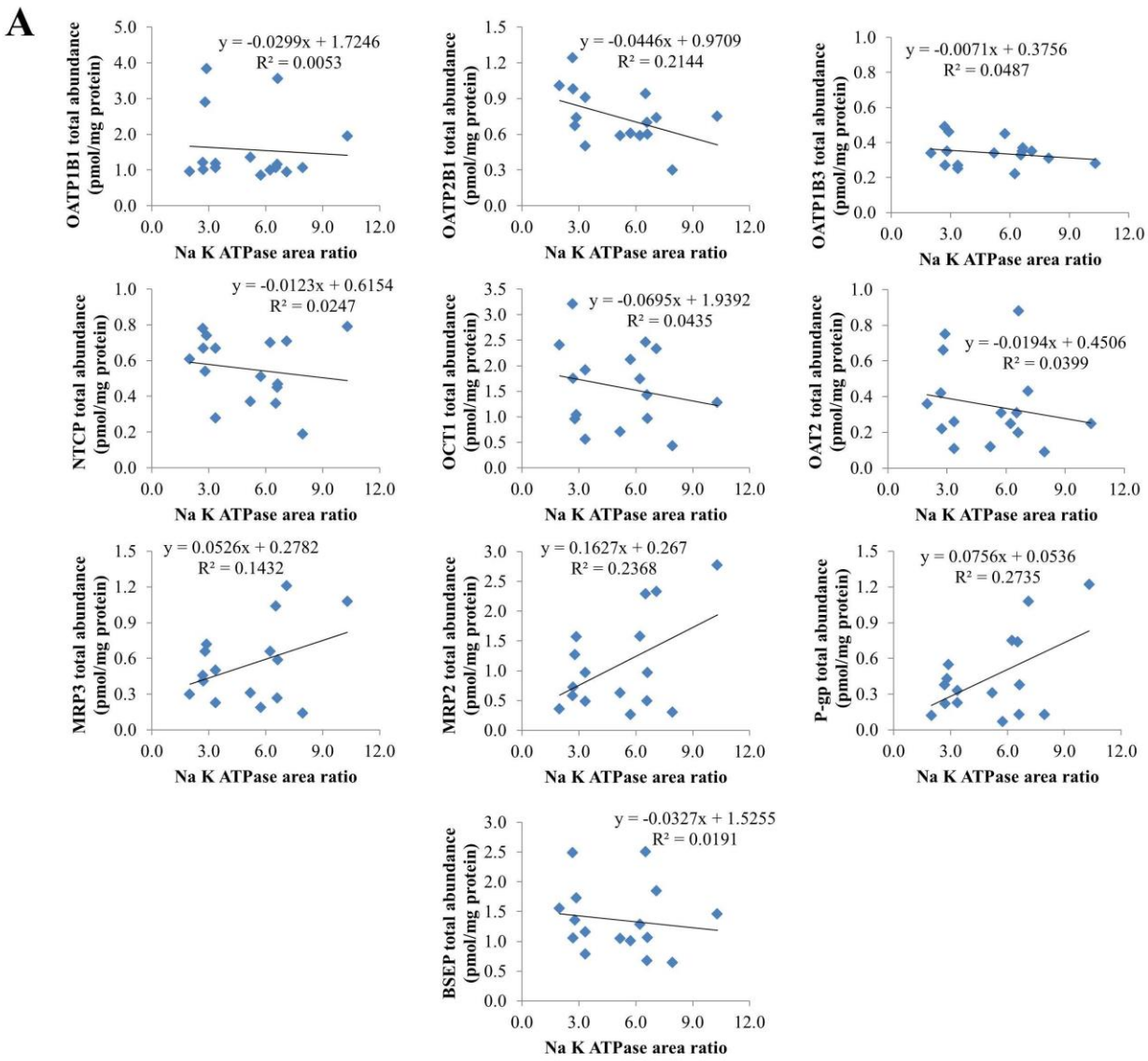

B

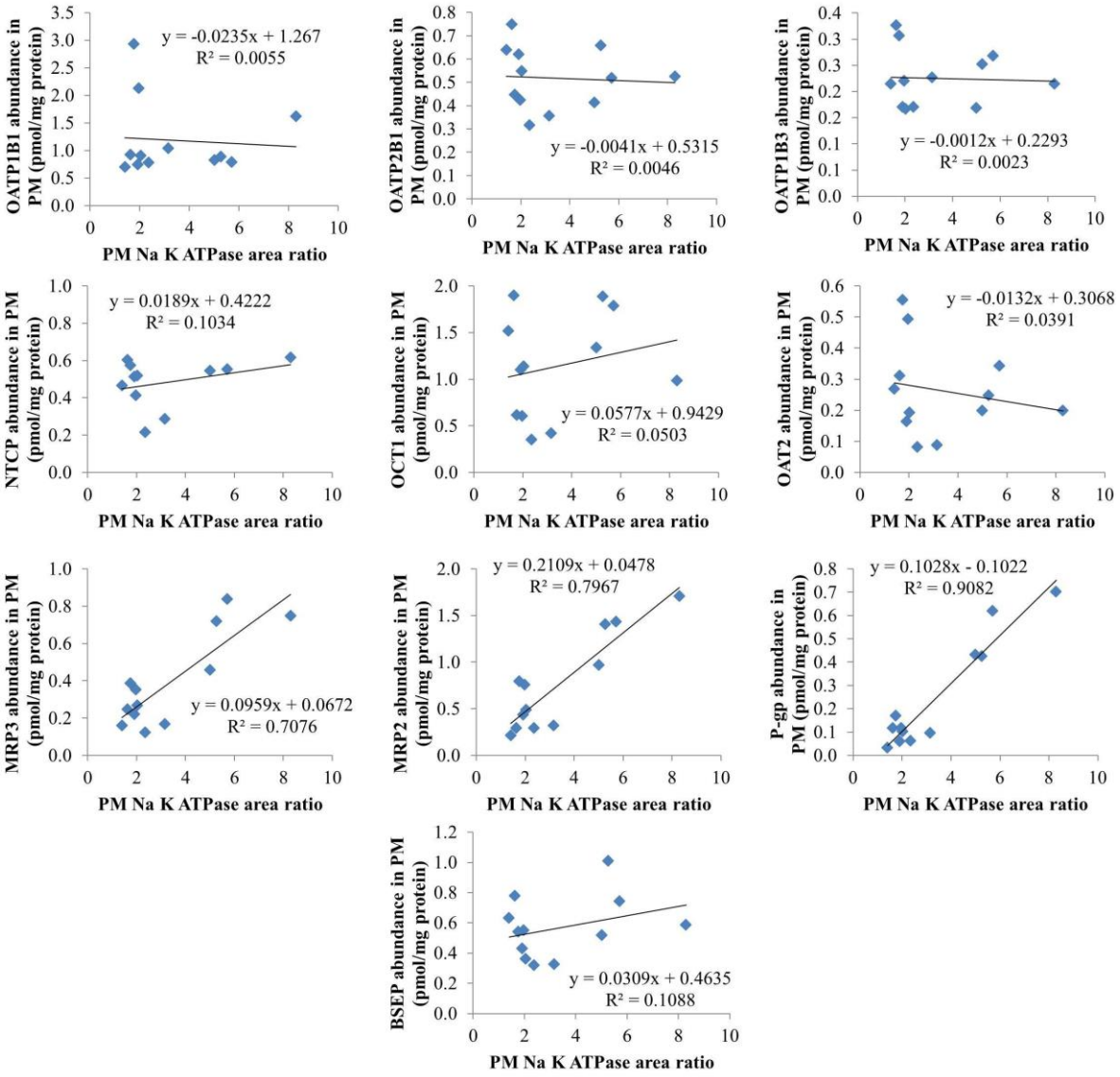
OATP1B1 abundance in PM (pmol/mg protein)
y = -0.0235x + 1.267
R² = 0.0055
PM Na K ATPase area ratio
OATP2B1 abundance in PM (pmol/mg protein)
y = -0.0041x + 0.5315
R² = 0.0046
PM Na K ATPase area ratio
OATP1B3 abundance in PM (pmol/mg protein)
y = -0.0012x + 0.2293
R² = 0.0023
PM Na K ATPase area ratio
NTCP abundance in PM (pmol/mg protein)
y = 0.0189x + 0.4222
R² = 0.1034
PM Na K ATPase area ratio
OCT1 abundance in PM (pmol/mg protein)
y = 0.0577x + 0.9429
R² = 0.0503
PM Na K ATPase area ratio
OAT2 abundance in PM (pmol/mg protein)
y = -0.0132x + 0.3068
R² = 0.0391
PM Na K ATPase area ratio
MRP3 abundance in PM (pmol/mg protein)
y = 0.0959x + 0.0672
R² = 0.7076
PM Na K ATPase area ratio
MRP2 abundance in PM (pmol/mg protein)
y = 0.2109x + 0.0478
R² = 0.7967
PM Na K ATPase area ratio
P-gp abundance in PM (pmol/mg protein)
y = 0.1028x - 0.1022
R² = 0.9082
PM Na K ATPase area ratio
BSEP abundance in PM (pmol/mg protein)
y = 0.0309x + 0.4635
R² = 0.1088
PM Na K ATPase area ratio

Supplemental Fig. 3.